Assessment of Extreme Precipitation in Future through Time-Invariant and Time-Varying Downscaling Approaches

Subbarao Pichuka [1] · Rajib Maity [1]

Abstract

Skill of a time-varying downscaling approach, namely Time-Varying Downscaling Model (TVDM), against time-invariant Statistical Downscaling Model (SDSM) approach for the assessment of precipitation extremes in the future is explored. The downscaled precipitation is also compared with a Regional Climate Model (RCM) product obtained from Coordinated Regional Climate Downscaling Experiment (CORDEX). The potential of downscaling the extreme events is assessed considering Bhadra basin in India as the study area through different models (SDSM, TVDM and RCM) during historical period (calibration: 1951–2005, testing: 2006–2012). Next, the changes in precipitation extremes during future period (2006–2035) have been assessed with respect to the observed baseline period (1971–2000), for different Representative Concentration Pathway (RCP) scenarios. All the models indicate an increasing trend in the precipitation, for the monsoon months and maximum increase is noticed using RCP8.5. The annual precipitation during the future period (RCP8.5) is likely to increase by 7.6% (TVDM) and 4.2% (SDSM) in the study basin. An increase in magnitude and number of extreme events during the future period is also noticed. Such events are expected to be doubled in number in the first quarter of the year (January–March). Moreover, the time-invariant relationship (in SDSM) between causal-target variables is needed to be switched with time-varying (TVDM). This study proves that the time-varying property in TVDM is more beneficial since its performance is better than SDSM and RCM outputs in identifying the extreme events during model calibration and testing periods. Thus, the TVDM is a better tool for assessing the extreme events.

✉ Rajib Maity
rajib@civil.iitkgp.ac.in

[1] Department of Civil Engineering, Indian Institute of Technology Kharagpur, Kharagpur, West Bengal 721302, India

1 Introduction

Climate change has a direct impact on the hydrologic cycle, which in turn affects the availability of the world's water resources (Arnell 1999; Mujumdar 2013; Taylor et al. 2013). However, its impact varies spatio-temporally depending upon the topographical and climatological features of the location (Maity and Kashid 2011; Gain and Wada 2014; Pichuka and Maity 2016; Amiri et al. 2016; Amiri and Mesgari 2016, 2017; Amiri et al. 2017; Amiri and Mesgari 2019). The climate change impact is not only restricted to the water resources sector but also spreads to the agricultural and industrial sectors (Kløve et al. 2014).

Furthermore, the impact of climate change on the extreme event of various hydrological variables is also a concern. For instance, Mishra and Singh (2010) have investigated the changes in extreme precipitation in Texas. The change in extreme rainfall events is expected in the hydrological systems along with the changes in the amount of average water availability (Jiang et al. 2007; Grillakis et al. 2016; Amiri and Mesgari 2018). Appropriate modelling and assessment of the mean as well as extreme events at local scale is of prime importance to forecast the agricultural production, local water resources, and epidemic outbreaks (Burn 1994; Lee and Bae 2015; He et al. 2016; Amiri and Mesgari 2017).

General Circulation Models (GCMs) help to simulate the future climate for different scenarios as defined by Intergovernmental Panel on Climate Change (IPCC) (Hewitson and Crane 1996). There are four possible climate change scenarios known as Representative Concentration Pathways (RCPs) adopted by IPCC. These are RCP2.6, RCP4.5, RCP6.0 and RCP8.5 respectively. The GCMs consider these scenarios and project the future climate variables. These projections are skillful in representing the global climate trends. However, the applicability of GCM outputs is restricted to coarse-scale resolution and are unsuitable for sub-grid scale impact assessment (Pichuka and Maity 2016). Thus, assessment of climate at sub-grid scale requires 'downscaling' methods that provide the information on spatial variability of different variables at smaller spatial scale.

The downscaling is divided into dynamical and statistical downscaling methods. Dynamical downscaling derives high-resolution regional data driven by low-resolution GCM outputs by relating numerical climatic modeling to reflect the effect of large-scale patterns on local conditions (Xue et al. 2014). The usage of dynamical downscaling is limited due to the complexity involved in its design and computationally high intensive (Xue et al. 2014). On the other hand, statistical downscaling methods convert the GCM output to local-scale data through a set of equations developed between causal and target variables (Rashid et al. 2015; Piras et al. 2016). It is computationally less demanding and with the reasonable output. However, this method assumes that the relationship between causal-target variable is time-invariant which is practically questionable under continuously changing climate and the physical features of the basin in terms of Land Use Land Cover (LULC) due to anthropogenic activities (Liu et al. 2017). Numerous studies have established the role of climate change and LULC on variation of several hydroclimatic parameters and their interdependency over a period of time (Cuo et al. 2011; Eum et al. 2016). It, therefore, opens to a

discussion with regard to the validity of stationary downscaling techniques based on the time-invariant relationship between the GCM outputs and basin scale hydroclimatic variables over large time periods (Vrac et al. 2007). The physical transformation of a basin over a certain time period can alter the association between hydroclimatic variables (Sarhadi et al. 2016). It means the relationship between causal-target variables is likely to be non-stationary (time-varying). Such a model has been developed by Pichuka and Maity (2018) and named as Time-Varying Downscaling Model (TVDM). The TVDM keeps the advantages of statistical down-scaling (computationally less intensive) but able to capture the non-stationarity in the causal and target variables. Thus, the objective of the present study is to explore the potential benefits of TVDM (time-varying) model with respect to the SDSM (time-invariant) and RCM downscaled precipitation in representing the extreme events. Towards this, the outputs from time-varying (TVDM and RCM) and time-invariant (SDSM) approaches are compared with each other. It is checked how far the non-stationary based approach is able to capture the extreme events better than stationary based approach? Next, the variation of these extreme events (number and magnitude) in the near future (2006–2035) is assessed at monthly and seasonal scales.

2 Materials and Methods

General methodological outline is shown in Fig. 1. Steps are discussed in details in the following subsections.

2.1 GCMs Used in this Study

The outputs from two GCMs are used in this study – the Beijing Climate Center Climate System Model, version 1.1 (BCCCSM1.1) and coupled Hadley centre Global Environmental Model (version-2) - Earth System model (HadGEM2-ES). The BCCCSM1.1 is developed at the Beijing Climate Center (BCC), China Meteorological Administration (CMA) it is a coupled atmosphere-ocean GCM (Xiaoge et al. 2013). The spatial resolution is 2.81° (lat.) × 2.81° (lon.) and the atmospheric components has 17 pressure levels. The HadGEM2-ES is developed at the Hadley centre in the UK meteorological office and the horizontal resolution is 1.25° (lat.) × 1.875° (lon.) with 38 pressure levels. The details of HadGEM2-ES can be found from Caesar et al. (2013).

2.2 RCM Used in this Study

The Hadley Centre Global Environmental Model version-3 regional climate model (HadGEM3-RA) RCM outputs are downloaded from the CORDEX web portal for historical and future periods from RCP4.5 and RCP8.5 scenarios. The horizontal resolution of HadGEM3 is 0.50° × 0.50° (lat. x lon.) and has atmospheric components of 19 levels. The RCM is developed at the met office Hadley center, UK and used by National Institute of Meteorological Research (NIMR), KMA, South Korea. The bias corrected outputs are pre-pared for the East Asian region by the NIMR and made available with CORDEX data. The HadGEM3-RA outputs are used for simulating the West African monsoon (Diallo et al. 2014). The details can be found elsewhere (Lee et al. 2012).
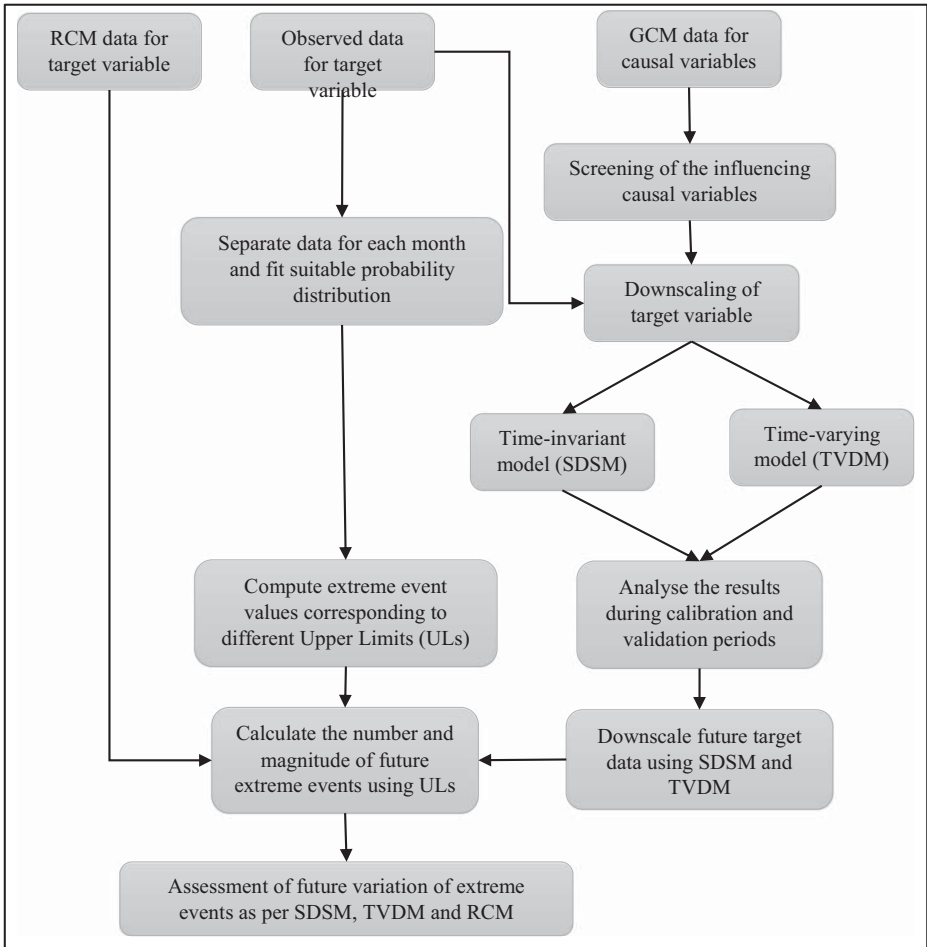
Fig. 1 Methodological flowchart showing overall outline of the approach

2.3 Statistical Downscaling Model (SDSM)

The SDSM is developed by Wilby et al. (2002) for downscaling the hydro-climatic variables to a point/local scale. The latest version of SDSM (SDSM-5.2) is used in this study for assessing the extreme rainfall events. As said earlier, the SDSM assumes the relationship between predictor-predictand variables as time-invariant. Moreover, the input data to be provided at each location manually. Therefore, to use this model for assessing the climate of a country at high spatial resolution ($0.25° \times 0.25°$) is very difficult and time consuming. Further details on SDSM can be found in Wilby et al. (2002) and Wilby and Dawson (2013).

2.4 Time-Varying Downscaling Model (TVDM)

TVDM is recently developed by considering the time-varying association between large scale (causal) variables and the target variable (Pichuka and Maity 2018). The

benefits of TVDM lies in the fact that it updates the predictor-predictand relationship at each time step which separates it from the other non-stationarity based approaches (Sachindra and Perera 2016; Merkenschlager et al. 2017). The benefits of TVDM over stationary based approach (i.e. SDSM) and non-stationary based approach (i.e. RCM) is explained in Pichuka and Maity (2018). However, the ability of TVDM in assessing the extreme rainfall events is the prime focus of this study.

2.5 Selection of Causal Variables

The selection of causal variables (large-scale atmospheric variables) is vital task in any downscaling approach as the skill of climate models are depends on it. In this study, the procedure used by Pichuka and Maity (2016) has been adopted for identifying the strong causal variables. The evaporation, surface specific humidity, upward latent heat flux, precipitation flux, zonal and meridional velocities at 500 hpa pressure levels are found to have better correlation with the observed precipitation in the Bhadra basin.

2.6 Extreme Event Analysis

At the outset, it can be noted that all the models run at monthly scale. However, for assessing the extreme events (at quarterly basis), the final output during the baseline period and future period is divided into 4 equal quarters in every year – January-February-March (JFM), April–May-June (AMJ), July–August-September (JAS) and October–November-December (OND). Then the quarter-wise data from the baseline period (1971–2000) are used to obtain the best fit distribution and corresponding cumulative distribution function (cdf). Different parametric distributions namely gamma, extreme value type-I and log-normal distributions are used. Reason for selecting non-parametric distribution is not to limit the range of precipitation within the historical observed value as the extreme values may increase by number as well as magnitude in future. The best-fit parametric distribution is identified using the log likelihood value. The highest log likelihood value indicates the best fit of the distribution. After selection the best-fit distribution, three sets of extreme thresholds or Upper Limits (ULs) are defined in this study, which are obtained from the cdf plot of the fitted distribution corresponding to 0.90 (90% UL), 0.95 (95% UL) and 0.99 (99% UL) quantile respectively. Then the number of events beyond these limits are counted for each of the thresholds during baseline as well as future periods. The assessment of extreme events during the future period is carried out and compared with the observed baseline precipitation.

3 Study Area and Data

The Bhadra river is considered as study basin as shown in Fig. 2. The river originates at Gangamoola in Varaha Parvatha in the Western Ghats range of Karnataka, India. The altitude of the Bhadra basin is about 1198 m and contains 1968 km^2 catchment area with an average slope of 6%. The average annual rainfall of Bhadra basin is 2320 mm and mostly received during the monsoon months (June through September).
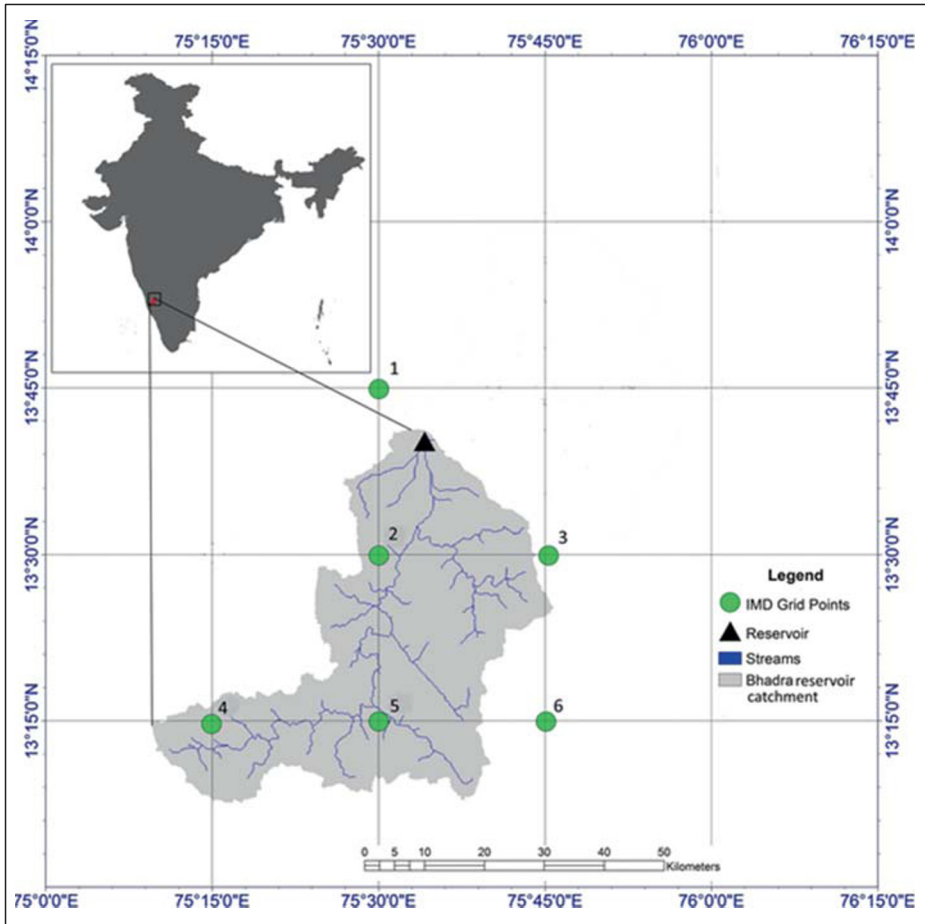
Fig. 2 Study area map

3.1 Data Description

The monthly precipitation data at a resolution of 0.25° × 0.25° (lat. × lon.) are acquired from India Meteorological Department (IMD), for the period of 1951–2013. The GCM outputs of large scale atmospheric variables are procured from the BCCCSM1.1 and HadGEM2-ES during the historical period (1951–2005). For the future period (2006–2035) these outputs are considered for different climate scenarios viz. RCP2.6, RCP4.5, RCP6.0 and RCP8.5. All these causal data are downloaded from the CMIP-5 web portal (http://www.ipcc-data.org/sim/gcm_monthly/AR5/Reference-Archive.html). The RCM data are obtained from the HadGEM3-RA RCM model supplied by the CORDEX web portal for the East Asian region (http://cordex-ea.climate.go.kr/cordex/). It can be noted that, the rawGCM and the RCM precipitation outputs at the required locations i.e. at the grid intersections of IMD data (shown in Fig.2) are computed by interpolation using Inverse Distance Weighting (IDW) method. Finally, both the data (observed and GCM) are used as input in SDSM and TVDM for downscaling the precipitation during the historical and future periods.

4 Results

The monthly precipitation is downscaled to finer grid size (0.25° × 0.25°) at all the grid intersections of observed precipitation in the Bhadra basin (shown in Fig. 2). It can be noted that the analysis is carried out after applying the bias correction to the model outputs (except rawGCM). The bias correction factors are calculated by dividing the long-term monthly means of downscaled and observed data. Then these bias correction factors are multiplied to the downscaled precipitation to obtain bias corrected values. The models are first calibrated for 55 years (1951–2005) against the observed precipitation data. Then, the future precipitation (2006–2035) is downscaled using causal-target relationship in case of SDSM; the regenerated causal-target relationship is used in case of TVDM. In the future period, the causal variables are used for different RCP scenarios viz. RCP2.6, RCP4.5, RCP6.0 and RCP8.5. The analysis is carried out at two temporal scales i.e. monthly and seasonal scales. The performance of the models (SDSM, TVDM and RCM) is evaluated through various statistical measures like mean (μ), standard deviation (σ), 5th, 25th, 75th, 90th and 95th percentile values. A part of the observed data (2006–2012) is kept aside to validate the capability of the downscaling models (validation period).

Overall, the analysis proves that the TVDM downscaled precipitation captures the observations very well (in mean, standard deviation and different percentile values). Figure 3 that presents Scatter plot between observed vs rawGCM rainfall (first panel), observed vs SDSM d/s rainfall (second panel), observed vs TVDM d/s rainfall (third panel) and observed vs RCM d/s rainfall (last panel), using HadGEM2-ES (left side) and BCCCSM1.1 (right side) GCM outputs. Left side figure indicates model calibration period (1951–2005) and right side figure represents model validation period (2006–2012). For brevity, scatterplots are presented at location-3 for demonstrating the results. The left side figures correspond to model calibration period (1951–2005) and right side ones indicate model validation period (2006–2012) respectively. Detailed model performance during during calibration (1951–2005) and validation (2006–2012) periods are presented in the supplementary document.

The analysis reveals better performance of TVDM (third-panel of Fig. 3 from both the GCMs and Table S1) as compared to the rawGCM (first-panel), SDSM (second-panel of Fig. 3 and Table S1) and RCM (fourth-panel of Fig. 3 and Table S1). The SDSM overestimates the low rainfall events and underestimates the peak values (second-panel of Fig. 3 and Table S1). As expected, the results are improved after downscaling as compared to the rawGCM precipitation which is poorly matching with the observations (first-panel of Fig. 3 and Table S1). The analysis reveals that the TVDM is superior to RCM and SDSM. It is also noteworthy that RCM performs better than the SDSM. It indicates the superiority of time-varying approach (TVDM and RCM) over time-invariant approach (SDSM) in assessing the extreme events.

4.1 Month-Wise Assessment of Future Precipitation

The monthly average precipitation over the Bhadra basin at all the locations for each month is shown in Table 1. An increase in mean is noticed in the future period as compared to the baseline period for all the monsoon months (except June in RCP2.6 and RCP6.0 scenarios). However, it is expected to be increased during the month of June as per the RCP4.5 and RCP8.5 (refer Table 1) using GCM1 (BCCCSM1.1) outputs as per TVDM. Increasing trend is also noticed using GCM2 (HadGEM2-ES) outputs except in June, where it is found to be decreased from all the RCP scenarios. The difference in reduction is more in case of SDSM
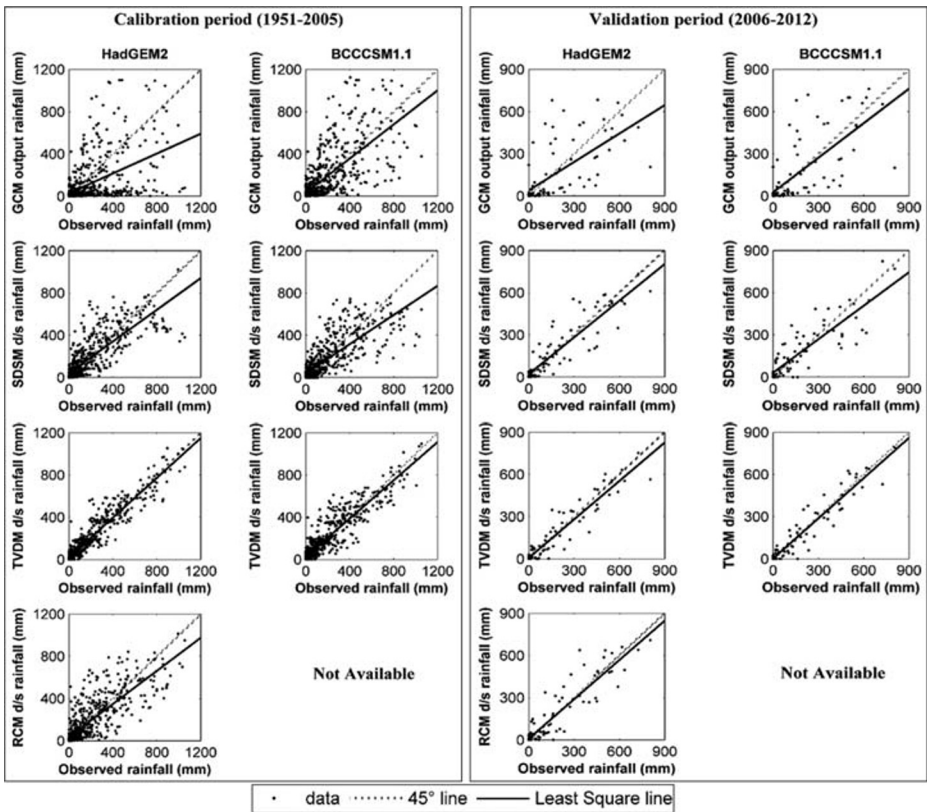
Fig. 3 Scatter plot between observed vs rawGCM precipitation (first panel), observed vs SDSM downscaled precipitation (second panel), observed vs TVDM downscaled precipitation (third panel) and observed vs RCM downscaled precipitation (last panel), using HadGEM2-ES (left side) and BCCCSM1.1 (right side) GCM outputs. Left side figure indicates model calibration period (1951–2005) and right side figure represents model validation period (2006–2012) respectively at location-3

than TVDM. The other monsoon months e.g. July, the precipitation (mm) is increased from 745.0 (baseline period) to 773.5 (RCP2.6), 773.2 (RCP4.5), 775.9 (RCP6.0) and 786.5 (RCP8.5) respectively as per TVDM output. The increment is found less in case of SDSM and RCM. Further, it is also reflected from the TVDM (Table 1) output that the increment during the monsoon months (June through September) is expected to be high in RCP8.5 as compared to the baseline period and other RCPs. The SDSM shows maximum increment (28.2%) in September as compared to the baseline period in RCP8.5 scenario using GCM2. The maximum increment during the months of March and May is found in RCP2.6 using GCM1 as per TVDM. The corresponding values in 'mm' during the future (baseline) period are 19.3 (9.0) in the March and 104.2 (89.9) during May. The maximum increment in the month of April are noted as 55.7 mm (GCM1) and 55.6 mm (GCM2) in RCP6.0 as compared to the baseline period (51.6 mm). The maximum increment is varying between all the RCPs across the different months. However, RCP8.5 is considered to be more critical as the monsoonal increment is very high. It can be noted that the increment in case of GCM2 (HadGEM2-ES) is consistently less as compared to the GCM1 (BCCCSM1.1) in the monsoon months (June through September).

Table 1 Month-wise mean precipitation values in the Bhadra basin during baseline period (1971–2000) and future period (2006–2035) considering various RCP scenarios with different downscaling models using BCCCSM1.1 (GCM1) and HadGEM2-ES (GCM2) outputs

| Mon | BL | TVDM downscaled in (mm) | | | | | | | | SDSM downscaled in (mm) | | | | | | | | RCM in (mm) | |
| | | RCP2.6 | | RCP4.5 | | RCP6.0 | | RCP8.5 | | RCP2.6 | | RCP4.5 | | RCP6.0 | | RCP8.5 | | RCP4.5 | RCP8.5 |
		GCM1	GCM2	GCM1	GCM2	GCM1	GCM2	GCM1	GCM2	GCM1	GCM2	GCM1	GCM2	GCM1	GCM2	GCM1	GCM2		
Jan	1.6	2.1	2.9	2.0	3.1	2.3	2.5	2.3	3.4	2.3	2.4	2.7	2.7	1.9	2.6	2.4	3.0	2.5	3.4
Feb	1.4	2.0	2.2	2.5	2.2	2.4	2.7	1.4	3.2	1.8	1.5	1.7	1.6	1.0	1.3	1.8	1.9	3.3	1.6
Mar	9.0	19.3	18.3	17.9	18.6	17.1	18.9	15.5	21.0	13.2	14.9	13.2	15.1	13.0	15.0	13.7	16.1	17.0	14.4
Apr	51.6	47.6	47.8	54.6	53.6	55.7	55.6	55.2	55.3	60.5	49.9	60.2	52.0	56.4	58.6	48.7	57.7	47.5	52.2
May	89.9	104.2	98.8	100.9	99.5	101.5	97.3	104.0	102.2	115.6	109.7	101.2	113.5	107.2	115.2	113.7	118.1	76.1	86.1
Jun	515.5	511.2	451.9	517.1	460.7	514.2	442.1	525.2	492.7	473.0	402.0	459.3	430.3	454.1	439.2	478.0	451.3	398.8	442.3
Jul	745.0	807.7	773.5	809.0	773.2	810.6	775.9	817.2	786.5	749.6	748.2	769.4	750.7	759.1	747.6	769.9	756.0	776.3	783.9
Aug	584.5	601.6	594.5	587.1	589.8	599.5	596.5	631.4	605.0	597.2	559.0	607.4	562.1	566.5	561.5	608.0	593.0	614.4	631.9
Sep	230.2	231.5	227.9	240.0	234.1	238.5	231.8	235.6	236.0	248.6	287.9	255.4	307.1	261.8	287.1	262.5	295.2	225.3	232.1
Oct	175.1	188.0	164.1	190.6	169.6	195.4	141.0	203.4	183.5	196.9	141.3	197.6	152.0	212.3	156.0	203.8	169.2	177.8	188.0
Nov	64.6	67.0	59.6	72.1	60.7	71.3	54.6	65.5	58.8	62.2	50.6	60.5	52.3	61.8	45.8	63.9	60.0	64.9	64.3
Dec	13.1	14.6	28.5	13.7	26.1	16.6	25.2	17.7	30.1	15.6	24.3	15.7	23.4	16.7	28.5	18.7	30.4	16.7	12.7

4.2 Seasonal Assessment of Extreme Precipitation Events during Future Period

The monthly precipitation during the future period is divided on a quarterly basis. Then the quarterly data are fitted to different distribution and the best-fit distribution is ascertained as mentioned in the methodology. The fitted CDFs are shown in Fig. 4. It is noticed that the gamma distribution is the best-fit for the first (JFM) and last (OND) quarters. The lognormal distribution is the best-fit for the pre-monsoon months i.e. second quarter (AMJ) and the extreme value type-I distribution best-fit to the monsoon months (JAS). The extreme precipitation events are recognized considering various ULs as defined in section 2.5 and the results are presented in Table 2. The results revealed that there will be more number of extreme events during the future period. For instance, the number of extreme values obtained from 90% UL are expected to be double during the first quarter of future period. These values are expected to increase from 12 (baseline period) to 21/24 (TVDM), 17/23 (SDSM) and 16 (RCM) respectively using BCCCSM1.1/HadGEM2-ES GCM outputs from RCP8.5 scenario. Similar increment in the extreme events are observed in case of 95th and 99th percentile values. The number of extreme events are expected to be reduce as per second quarter (AMJ) i.e. summer months. However the magnitude of these events are increasing during the future period as compared to baseline period. For instance, it can be depicted from Table 2 that, the extreme events at 90% UL are noticed as 14 (baseline) which are expected to be reduced to 12 (TVDM) in RCP8.5 scenario, but their mean (680.9 mm) is increasing upto 2.7% as compared to the mean (663.0 mm) of baseline period using BCCCSM1.1 outputs. These values for 95% UL are reduced from 5 (baseline period) to 4 (TVDM and SDSM) and the mean of such events are 826.1 mm (baseline period) and 853.6 mm (TVDM) and 836.7 mm (SDSM). It can be
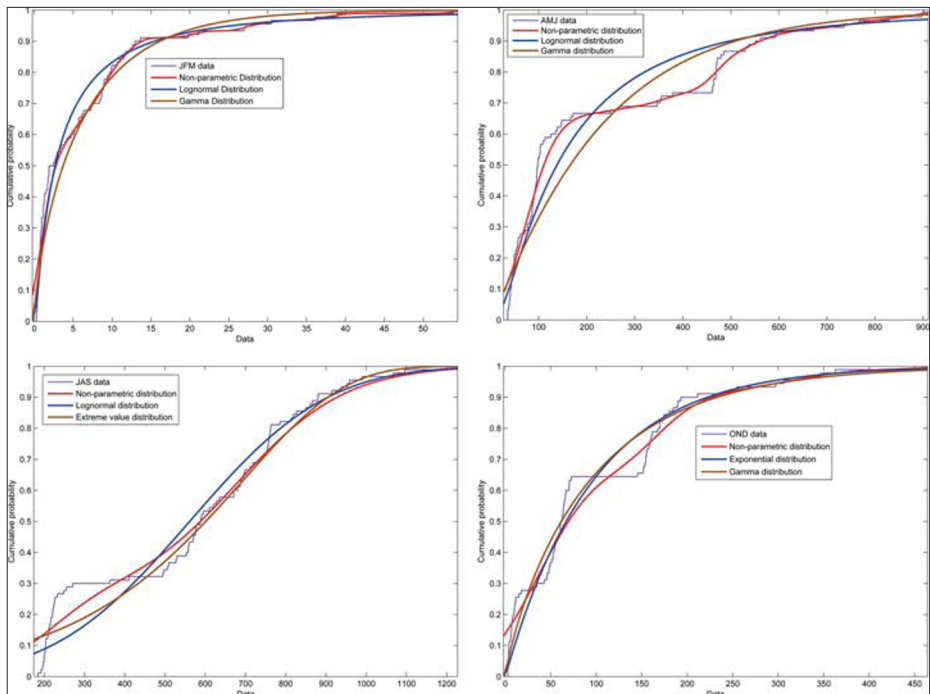

Fig. 4 CDF plots for seasonal analysis

noteworthy that the number of extreme events is higher in the other RCPs also. For instance, 95% UL of TVDM in RCP2.6 is 6 in second quarter (AMJ) the same UL in the third quarter (JAS) is observed as 4 in RCP4.5 using BCCCSM1.1 as per SDSM. Overall, the number of extreme events are expected to be doubled in the first quarter it is revealed from all the downscaling models and all RCPs.

Apart from this, the mean of extreme events is projected to be higher in RCP8.5 in all the quarters from TVDM. For instance, the mean of extreme events in 90% UL of each quarter during the baseline period (RCP8.5 using BCCCSM1.1 and HadGEM2-ES) is noted in 'mm' as 18.8 (19.5 and 22.4), 663.0 (680.9 and 700.5), 1015.9 (1016.8 and 1059.9) and 302.6 (324.9 and 288.2) respectively. The mean of extreme events in 95% UL corresponding to baseline (TVDM downscaled RCP8.5 scenario using BCCCSM1.1 and HadGEM2-ES) are noted in 'mm' as 21.3 (25.5 and 26.2), 826.1 (826.4 and 766.9), 1133.7 (1128.6 and 1134.6) and 332.0 (349.8 and 319.9) respectively. The similar observations are made in RCM output.

Further, the mean (standard deviation) of these quarterly months is calculated and presented in Table 3. The mean values are increasing in RCP8.5 when compared to the baseline period as per TVDM output in all the quarters and as per SDSM outputs during last two quarters (JAS and OND). Such values in 'mm' during the baseline period (RCP8.5 using BCCCSM1.1 and HadGEM2-ES) are obtained as 4.0 (7.3 and 7.6), 219.0 (228.1 and 224.5), 519.9 (561.4 and 557.2) and 84.3 (96.5 and 88.9) respectively in each quarter as per TVDM outputs. The similar observations made in the RCM output. The SDSM model produces slightly different in the even quarters (2nd and 4th) in case of BCCCSM1.1 according to these, the critical values are observed in RCP2.6 (216.4 mm) and RCP 6.0 (96.9 mm) respectively in respective quarters. However, during the monsoon months, the future precipitation is expected to be increased highly in RCP8.5 (544.5 mm). On the other hand, HadGEM2-ES shows critical (maximum magnitudes) values in RCP8.5 scenario in all the quarters. The variation of standard deviation values between baseline period and future period are also presented in Table 3. The standard deviation values are expected to be minimum during future period than baseline period.

5 Discussions

It is clear for the results that the time-varying concept based approach, TVDM, performs better than the SDSM and RCM in representing the mean values. It is even more explicit for the extreme values since the higher side extreme values are represented very well in TVDM output. The TVDM is able to capture the extremes far better than SDSM and RCM. It is also clear that the RCM performance is better than the SDSM, however its performance is found to be inferior when compared to the TVDM. This analysis proved the fact that the causal-target relationship is indeed time-varying (non-stationary). Therefore, it is understood that the TVDM will be the most suitable model for assessing the future extremes.

The month-wise assessment of future precipitation indicates an increase in mean in the future period as compared to the baseline period. The magnitude of increase during the future period with respect to baseline period is consistent in both the GCMs in almost all the months (except June and November). There will be wetter monsoon during the future period and the pre and post monsoon months are more or less expected to be same alike baseline period. The magnitude of precipitation during winter months is expected to be doubled. For instance, the magnitude of January precipitation is 1.6 mm during the baseline period, which is expected to increase upto 3.4 mm (TVDM), 3.0 mm (SDSM) and 3.4 mm (RCM) using GCM2.

Table 2 Number of extreme events (mean value of such events in 'mm') in baseline period (1971–2000) and future period (2006–2035) considering various RCP scenarios with respect to various Upper Limits (ULs) and different downscaling models using BCCCSM1.1 and HadGEM2-ES outputs

Model	Season	UL	Value (mm)	Baseline period	TVDM downscaled (future)				SDSM downscaled (future)
					RCP 2.6	RCP 4.5	RCP 6.0	RCP 8.5	RCP 2.6
BCCCSM1.1	JFM	90	9.13	12 (18.8)	24 (20.2)	25 (20.1)	26 (18.6)	21 (19.5)	19 (19.6)
		95	11.87	9 (21.3)	23 (22.3)	21 (21.8)	22 (20)	12 (25.5)	13 (24.2)
		99	18.26	3 (34.7)	13 (30.1)	9 (31.2)	10 (27.1)	8 (31.8)	7 (32.4)
	AMJ	90	519.89	14 (663.0)	10 (668.6)	10 (670.8)	10 (670.9)	12 (680.9)	9 (642.5)
		95	692.30	5 (826.1)	6 (763.8)	5 (776.9)	4 (789.5)	5 (826.4)	4 (753.6)
		99	1105.4	0 (0)	0 (0)	0 (0)	0 (0)	0 (0)	0 (0)
	JAS	90	901.66	11 (1015.9)	8 (1014.0)	8 (1027.1)	8 (1018.3)	8 (1036.8)	8 (1009.9)
		95	1032.0	2 (1133.7)	3 (1116.5)	3 (1127.0)	2 (1114.3)	3 (1138.6)	4 (1092.8)
		99	1286.7	0 (0)	0 (0)	0 (0)	0 (0)	0 (0)	0 (0)
	OND	90	211.5	7 (302.6)	5 (294.8)	6 (305.6)	7 (304.4)	8 (324.9)	10 (277.1)
		95	266.2	5 (332.0)	3 (341.6)	4 (332.4)	5 (328.6)	6 (349.8)	4 (324.5)
		99	374.1	1 (398.4)	1 (389.1)	1 (396.9)	1 (418.1)	1 (459.4)	1 (398.9)
HadGEM2-ES	JFM	90	9.13	12 (18.8)	26 (22.1)	22 (24.1)	24 (21.7)	24 (22.4)	21 (18.2)
		95	11.87	9 (21.3)	15 (24.5)	16 (27.8)	17 (25.6)	16 (26.2)	15 (21.5)
		99	18.26	3 (34.7)	12 (30.3)	12 (32.5)	13 (29.3)	13 (29.6)	8 (32.7)
	AMJ	90	519.89	14 (663.0)	8 (641.7)	8 (679.9)	9 (693.9)	10 (700.5)	8 (661.0)
		95	692.30	5 (826.1)	5 (706.1)	5 (741.3)	5 (765.5)	5 (766.9)	3 (782.9)
		99	1105.4	0 (0)	0 (0)	0 (0)	0 (0)	0 (0)	0 (0)
	JAS	90	901.66	11 (1015.9)	6 (1004.2)	7 (1023.6)	7 (1025.3)	8 (1049.9)	6 (1009.9)
		95	1032.0	2 (1133.7)	2 (1092.9)	2 (1126.8)	2 (1121.8)	3 (1134.6)	3 (1078.3)
		99	1286.7	0 (0)	0 (0)	0 (0)	0 (0)	0 (0)	0 (0)
	OND	90	211.5	7 (302.6)	4 (285.3)	5 (277.3)	5 (288.8)	6 (288.2)	6 (298.1)
		95	266.2	5 (332.0)	2 (318.9)	3 (313.6)	3 (320.8)	3 (319.9)	4 (326.7)
		99	374.1	1 (398.4)	0 (0)	1 (389.0)	1 (397.5)	1 (412.5)	1 (414.1)

Model	SDSM downscaled (future)	
	RCP	RCP

Model	RCM	
	RCP	RCP

Table 2 (continued)

Model	SDSM downscaled (future)			RCM	
	RCP 4.5	RCP 6.0	RCP 8.5	RCP 4.5	RCP 8.5
BCCCSM1.1	19 (18.6)	19 (18.4)	17 (20.8)	21 (22.8)	16 (22.6)
	14 (21.6)	12 (23.0)	13 (24.1)	14 (29.1)	14 (24.3)
	8 (26.9)	7 (28.4)	8 (30.7)	11 (31.8)	8 (31.7)
	9 (655.5)	8 (665.5)	11 (662.2)	9 (670.1)	9 (676.7)
	4 (778.2)	3 (836.3)	4 (809.8)	3 (836.7)	3 (831.1)
	0 (0)	0 (0)	0 (0)	0 (0)	0 (0)
	8 (1010.7)	8 (1018.0)	9 (1025.9)	8 (1001.1)	9 (1013.3)
	3 (1101)	3 (1128.0)	3 (1131.0)	3 (1109.7)	3 (1095.4)
	0 (0)	0 (0)	0 (0)	0 (0)	0 (0)
	11 (309.7)	14 (286.9)	13 (293.4)	12 (272.3)	8 (322.2)
	8 (341.5)	8 (324.8)	8 (328.5)	4 (329.4)	5 (363.6)
	1 (429.1)	1 (419.9)	1 (426.1)	1 (381.4)	2 (454.6)
HadGEM2-ES	22 (18.5)	22 (19.0)	23 (19.2)	21 (22.8)	16 (22.6)
	16 (21.8)	16 (22.7)	16 (23.9)	14 (29.1)	14 (24.3)
	9 (29.2)	8 (32.3)	9 (31.6)	11 (31.8)	8 (31.7)
	9 (670.9)	8 (681.1)	10 (727.5)	9 (670.1)	9 (676.7)
	4 (784.6)	4 (783.6)	5 (821.3)	3 (836.7)	3 (831.1)
	0 (0)	0 (0)	0 (0)	0 (0)	0 (0)
	7 (1010.7)	6 (1031.7)	8 (1038)	8 (1001.1)	9 (1013.3)
	3 (1079.8)	4 (1111.6)	5 (1112.9)	3 (1109.7)	3 (1095.4)
	0 (0)	0 (0)	0 (0)	0 (0)	0 (0)
	8 (289.3)	8 (287.1)	9 (271.8)	12 (272.3)	8 (322.2)
	5 (323.6)	5 (317.4)	5 (298.4)	4 (329.4)	5 (363.6)
	1 (429.3)	1 (411.6)	1 (381.7)	1 (381.4)	2 (454.6)

Table 3 Quarterly mean values (standard deviation) in 'mm' in the Bhadra basin during baseline period (1971–2000) and future period (2006–2035) considering various RCP scenarios with respect to various downscaling models using BCCCSM1.1 and HadGEM2-ES outputs

Model	Season	Baseline Period (1971–2000)	TVDM downscaled (2006–2035)				SDSM downscaled (2006–2035)
			RCP2.6	RCP4.5	RCP6.0	RCP8.5	RCP2.6
BCCCSM1.1	JFM	4.0 (7.4)	6.8 (10.3)	7.5 (10.0)	7.3 (8.5)	7.3 (9.8)	5.8 (9.5)
	AMJ	219.0 (239.8)	221.0 (220.6)	224.2 (222.6)	223.8 (220.7)	228.1 (233.3)	216.4 (212.5)
	JAS	519.9 (281.1)	547.0 (263.0)	548.7 (266.6)	549.5 (263.4)	561.4 (267.9)	535.1 (269.1)
	OND	84.3 (88.9)	89.9 (82.1)	92.1 (85.3)	94.4 (88.1)	96.5 (96.7)	91.6 (90.7)
HadGEM2-ES	JFM	4.0 (7.4)	6.7 (10.2)	7.5 (10.7)	7.4 (10.8)	7.6 (10.4)	6.8 (8.9)
	AMJ	219.0 (239.8)	215.8 (214.6)	217.9 (225.6)	209.1 (220.7)	224.5 (233.3)	204.3 (187.3)
	JAS	519.9 (281.1)	538.6 (250.8)	541.4 (253.4)	544.6 (243.4)	557.2 (269.8)	534.0 (221.1)
	OND	84.3 (88.9)	84.6 (72.1)	84.3 (75.2)	84.6 (78.1)	88.9 (81.2)	81.6 (79.1)

Model	SDSM downscaled (2006–2035)			RCM (2006–2035)	
	RCP4.5	RCP6.0	RCP8.5	RCP4.5	RCP8.5
BCCCSM1.1	5.9 (7.9)	5.3 (8.1)	6.0 (9.0)	7.6 (10.9)	7.5 (10.6)
	201.3 (197.7)	204.9 (205.0)	215.6 (217.0)	173.3 (208.5)	193.5 (215.1)
	544.0 (267.6)	529.8 (262.1)	544.5 (267.3)	538.7 (287.4)	549.3 (277.0)
	91.3 (99.8)	96.9 (99.5)	95.4 (97.6)	86.5 (91.9)	88.3 (96.3)
HadGEM2-ES	6.7 (8.6)	6.5 (9.3)	6.9 (9.5)	7.6 (10.9)	7.5 (10.6)
	211.3 (200.7)	201.7 (194.0)	215.3 (226.3)	173.3 (208.5)	193.5 (215.1)
	543.3 (234.4)	538.2 (224.6)	546.2 (273.8)	538.7 (287.4)	549.3 (277.0)
	86.0 (83.0)	83.6 (81.1)	87.9 (90.4)	86.5 (91.9)	88.3 (96.3)

The overall analysis of monthly precipitation data revealed that the future precipitation during the monsoon months are expected to be increased as compared to the baseline period. The increment is maximum in case of RCP8.5 scenario. The TVDM downscaled precipitation shows highest increment and it can be reliable since it outperformed SDSM and RCM during the historical period.

The results related to seasonal assessment of extreme precipitation events during future period reveal a fact that though the number of extreme events are more or less same, the magnitude of such events are severe in case of RCP8.5. The number of extreme events and their magnitude will be higher in the future period when compared to the baseline period as per TVDM. It is worth mentioning that incorporation of time-varying term in the causal-target relationship is the prime reason behind the accurate assessment of extreme events by TVDM as compared to the SDSM.

Overall, it can be commented that the extreme events during future period are expected to increase not only in number but also their magnitudes. The increment is severe as per the TVDM and the results drag more attention due to the outstanding performance of TVDM in recognizing the extreme events during the historical period (where the observed data is available). Therefore, the time-varying (TVDM) approach is more reliable for assessing the extreme events as compared to the time-invariant (SDSM) approach.

6 Conclusions

The present study explores the potential benefits of time-varying downscaling approach (e.g. TVDM) over time invariant approach (e.g. SDSM) for the assessment of extreme events in particular. The variation of monthly precipitation during the future period is also assessed. The Bhadra basin in Karnataka, India is considered for demonstration. A comparative analysis among time-invariant (SDSM) and time-varying (TVDM and RCM) downscaling approaches is carried out using multiple GCM outputs. For all the cases, the future results (2006–2035) are compared with the observed baseline data (1971–2000). The important findings from this study are summarized as follows.

The monthly and seasonal time scales are considered for the temporal impact assessments over the Bhadra basin. The TVDM showed exceptional performance in reproducing the observed precipitation values during the calibration and validation periods as compared to SDSM and RCM. In particular, the superiority of TVDM over other models is lies in identifying the extreme events during historical period, which are closely match with the observations. All the models perform with more or less equal merit in representing the mean values.

At monthly scale, the future downscaled precipitation shows an increasing trend in all the RCPs and high during the monsoon months (July–September). The maximum increment, in particular, is taking place in RCP8.5 and is observed in all the models. However, the increment during dry months is varying from model to model but, they have clearly shown an increasing trend in all the RCPs during the pre-monsoon months (February–May). The post-monsoon months (October–January) have also shown similar trends as far as TVDM output is concerned.

The number of extreme events during future period are expected to be doubled during the first quarter (January–March), they are not changing much in the second quarter (April–June). The third quarter (July–September) shows that the number and magnitude of high extreme events (95th percentiles) will be more during the future period. It (high magnitudes) indicates that the occurrence of severe floods is more likely in the near future.

Overall it can be concluded that there will be more 'wetter' months (increase of monthly precipitation amounts) during the future period (2006–2035) when compared to the baseline period (1971–2000). It will be severe in RCP8.5 scenario as compared to other scenarios. The increment (effect of wetness) is expected to be more as per the time-varying (TVDM) model than time-invariant SDSM.

The consistency in the results are observed from both GCMs used in this study except slight changes in the monthly precipitation. It is may be due to the Bhadra basin lies in the high rainfall region, and possibly both the GCMs are performing consistently at these regions. It implies that the selection of GCM does not hamper the analysis as far as Bhadra basin is concern.

In brief, the time-varying (TVDM) approach is the better choice in the regional scale impact studies because of the time-varying nature of the causal-and-target-variable (when compared against SDSM), reduced computational costs (when compared against RCM) and higher accuracy. Thus the TVDM approach is more comprehensive and can be applied to any basin around the world to assess the local climate change. Thus, the newly developed downscaling technique (TVDM) can be utilized to downscale various hydroclimatic variables like temperature, soil moisture, and evaporation; at point and local scales is kept as future scope of this work.

Compliance with Ethical Standards

Conflict of Interest None.

References

Amiri MA, Mesgari MS (2016) Spatial variability analysis of precipitation in Northwest Iran. Arab J Geosci 9(11):578–510. https://doi.org/10.1007/s12517-016-2611-7

Amiri MA, Mesgari MS (2017) Modeling the spatial and temporal variability of precipitation in Northwest. Iran. Atmosphere 8(12: 254):1–14. https://doi.org/10.3390/atmos8120254

Amiri MA, Mesgari MS (2018) Improving the accuracy of rainfall prediction using a regionalization approach and neural networks. Kuwait Journal of Science 45(4):66–75

Amiri MA, Mesgari MS (2019) Spatial variability analysis of precipitation and its concentration in Chaharmahal and Bakhtiari province. Iran Theoretical and Applied Climatology 137:2905–2914. https://doi.org/10.1007/s00704-019-02787-y

Amiri MA, Amerian Y, Mesgari MS (2016) Spatial and temporal monthly precipitation forecasting using wavelet transform and neural networks, Qara-Qum catchment, Iran. Arab J Geosci 9(5):1–18. https://doi.org/10.1007/s12517-016-2446-2

Amiri MA, Mesgari MS, Conoscenti C (2017) Detection of homogeneous precipitation regions at seasonal and annual time scales, Northwest Iran. Journal of Water and Climate Change 8(4):701–714. https://doi.org/10.2166/wcc.2017.088

Arnell NW (1999) Climate change and global water resources. Glob Environ Chang 9:S31–S49

Burn DH (1994) Hydrologic effects of climatic change in west-Central Canada. J Hydrol 1694:53–70. https://doi.org/10.1016/0022-1694(94)90033-7

Caesar J, Palin E, Liddicoat S et al (2013) Response of the HadGEM2 earth system model to future greenhouse gas emissions pathways to the year 2300. J Clim:3275–3284. https://doi.org/10.1175/JCLI-D-12-00577.1

Cuo L, Beyene TK, Voisin N et al (2011) Effects of mid-twenty-first century climate and land cover change on the hydrology of the Puget Sound basin. Washington Hydrological Processes doi. https://doi.org/10.1002/hyp.7932

Diallo I, Bain CL, Gaye AT et al (2014) Simulation of the west African monsoon onset using the HadGEM3-RA regional climate model. Clim Dyn 43:575–594. https://doi.org/10.1007/s00382-014-2219-0

Eum H, Dibike Y, Prowse T (2016) Comparative evaluation of the effects of climate and land-cover changes on hydrologic responses of the Muskeg River, Alberta, Canada. Journal of Hydrology: Regional Studies 8:198–221. https://doi.org/10.1016/j.ejrh.2016.10.003

Gain AK, Wada Y (2014) Assessment of future water scarcity at different spatial and temporal scales of the Brahmaputra River basin. Water Resour Manag 28:999–1012. https://doi.org/10.1007/s11269-014-0530-5

Grillakis MG, Koutroulis AG, Komma J et al (2016) Initial soil moisture effects on flash flood generation – a comparison between basins of contrasting hydro-climatic conditions. J Hydrol. https://doi.org/10.1016/j.jhydrol.2016.03.007

He X, Chaney NW, Schleiss M, Sheffield J (2016) Spatial downscaling of precipitation using adaptable random forests. Water Resour Res 52:8217–8237. https://doi.org/10.1002/2016WR019034

Hewitson BC, Crane RG (1996) Climate downscaling : techniques and application. Clim Res 7:85–95

Jiang T, Chen DY, Xu C et al (2007) Comparison of hydrological impacts of climate change simulated by six hydrological models in the Dongjiang Basin, South China. J Hydrol 336:316–333. https://doi.org/10.1016/j.jhydrol.2007.01.010

Kløve B, Ala-aho P, Bertrand G et al (2014) Climate change impacts on groundwater and dependent ecosystems. J Hydrol 518:250–266. https://doi.org/10.1016/j.jhydrol.2013.06.037

Lee MH, Bae DH (2015) Climate change impact assessment on green and blue water over Asian monsoon region. Water Resour Manag 29:2407–2427. https://doi.org/10.1007/s11269-015-0949-3

Lee I. H, Park S. H, Kang H. S, Cho C. H (2012) Regional climate projections using the HadGEM3-RA. 3rd international conference on earth system Modelling. Korea,

Liu J, Zhang C, Kou L, Zhou Q (2017) Effects of climate and land use changes on water resources in the Taoer River. Advances in Meterology. https://doi.org/10.1155/2017/1031854

Maity R, Kashid SS (2011) Importance analysis of local and global climate inputs for basin-scale streamflow prediction. Water Resour Res 47:1–17. https://doi.org/10.1029/2010WR009742

Merkenschlager C, Hertig E, Jacobeit J (2017) Non-stationarities in the relationships of heavy precipitation events in the Mediterranean area and the large-scale circulation in the second half of the 20th century. Glob Planet Chang 151:108–121. https://doi.org/10.1016/j.gloplacha.2016.10.009

Mishra AK, Singh VP (2010) Changes in extreme precipitation in Texas. J Geophys Res. https://doi.org/10.1029/2009JD013398

Mujumdar PP (2013) Climate change: a growing challenge for water Management in Developing Countries. Water Resour Manag 27:953–954. https://doi.org/10.1007/s11269-012-0223-x

Pichuka S, Maity R (2016) Spatio-temporal downscaling of projected precipitation in 21st century : indication of a wetter monsoon over the upper Mahanadi basin in India. Hydrol Sci J. https://doi.org/10.1080/02626667.2016.1241882

Pichuka S, Maity R (2018) Development of a time-varying downscaling model considering non-stationarity using a Bayesian approach. International Journal of Climatology. doi, Accepted

Piras M, Mascaro G, Deidda R, Vivoni ER (2016) Impacts of climate change on precipitation and discharge extremes through the use of statistical downscaling approaches in a Mediterranean basin. Sci Total Environ 543:952–964. https://doi.org/10.1016/j.scitotenv.2015.06.088

Rashid M, Beecham S, Chowdhury RK (2015) Statistical downscaling of rainfall : a non-stationary and multi-resolution approach. Theor Appl Climatol 124:919–933. https://doi.org/10.1007/s00704-015-1465-3

Sachindra DA, Perera BJC (2016) Statistical downscaling of general circulation model outputs to precipitation accounting for non-Stationarities in predictor-Predictand relationships. PLOSone 11:1–21. https://doi.org/10.1371/journal.pone.0168701

Sarhadi A, Ausín MC, Wiper MP (2016) A new time-varying concept of risk in a changing climate. Nat Sci Rep 6:1–7. https://doi.org/10.1038/srep35755

Taylor RG, Scanlon B, Doll P et al (2013) Ground water and climate change. Nat Clim Chang 3:322–329. https://doi.org/10.1038/NCLIMATE1744

Vrac M, Stein ML, Hayhoe K, Liang X (2007) A general method for validating statistical downscaling methods under future climate change. Geophys Res Lett 34:1–5. https://doi.org/10.1029/2007GL030295

Wilby RL, Dawson CW (2013) The statistical DownScaling model: insights from one decade of application. Int J Climatol 33:1707–1719. https://doi.org/10.1002/joc.3544

Wilby RL, Dawson CW, Barrow EM (2002) SDSM — a decision support tool for the assessment of regional climate change impacts. Environ Model Softw 17:145–157. https://doi.org/10.1016/S1364-8152(01)00060-3

Xiaoge X, Tongwen W, Jianglong L et al (2013) How Well does BCC _ CSM1 . 1 Reproduce the 20th Century Climate Change over China ? Atmospheric and Oceanic Science Letters 2834:20–26. https://doi.org/10.1080/16742834.2013.11447053

Xue Y, Janjic Z, Dudhia J et al (2014) A review on regional dynamical downscaling in intraseasonal to seasonal simulation/prediction and major factors that affect downscaling ability. Atmos Res 147–148:68–85. https://doi.org/10.1016/j.atmosres.2014.05.001